Generation of pronounced Fano resonances and tuning of subwavelength spatial light distribution in plasmonic pentamers

M. Rahmani,[1,2] B. Lukiyanchuk,[1] B. Ng,[1,3] A. Tavakkoli K. G.,[1,4] Y. F. Liew[1,2] and M.H. Hong[1,2,*]

[1]*Data Storage Institute, (A*STAR) Agency for Science Technology and Research, 5 Engineering Drive 1, 117608 Singapore*

[2]*Department of Electrical and Computer Engineering, National university of Singapore, 4 Engineering Drive3, 117576 Singapore*

[3]*Experimental Solid State Group, Physics Department, Imperial College London, London SW7 2AZ, UK*

[4]*NUS graduate school for integrative sciences and Engineering, National university of Singapore, 28 Medical Drive, 117456 Singapore*

**elehmh@nus.edu.sg*

Abstract: Arrays of plasmonic pentamers consisting of five metallic nano-disks were designed and fabricated to achieve a pronounced Fano Resonance with polarization-independent far-field spectral response at normal incidence due to the structure symmetry of pentamers. A mass-spring coupled oscillator model was applied to study plasmon interactions among the nano-disks. It was found that the direction of the excitation light polarization can flexibly tune the spatial localization of near-field energy at sub-wavelength scales while the collective optical properties are kept constant. It can lead to a selective storage of excited energy down to sub-20 nm gap at a normal incident with a single light source.

OCIS codes: (310.6628) Subwavelength structures, nanostructures; (240.6680) Surface plasmons; (260.5740) Resonance; (240.5445) Polarization-selective devices.

References and links

1. B. Luk'yanchuk, N. I. Zheludev, S. A. Maier, N. J. Halas, P. Nordlander, H. Giessen, and C. T. Chong, "The Fano resonance in plasmonic nanostructures and metamaterials," Nat. Mater. **9**(9), 707–715 (2010).
2. A. E. Miroshnichenko, S. Flach, and Y. S. Kivshar, "Fano resonances in nanoscale structures," Rev. Mod. Phys. **82**(3), 2257–2298 (2010).
3. N. Verellen, Y. Sonnefraud, H. Sobhani, F. Hao, V. V. Moshchalkov, P. Van Dorpe, P. Nordlander, and S. A. Maier, "Fano resonances in individual coherent plasmonic nanocavities," Nano Lett. **9**(4), 1663–1667 (2009).
4. N. Berkovitch, P. Ginzburg, and M. Orenstein, "Concave plasmonic particles: broad-band geometrical tunability in the near-infrared," Nano Lett. **10**(4), 1405–1408 (2010).
5. J. A. Fan, C. Wu, K. Bao, J. Bao, R. Bardhan, N. J. Halas, V. N. Manoharan, P. Nordlander, G. Shvets, and F. Capasso, "Self-assembled plasmonic nanoparticle clusters," Science **328**(5982), 1135–1138 (2010).
6. Y. S. Joe, A. M. Satanin, and C. S. Kim, "Classical analogy of Fano resonances," Phys. Scr. **74**(2), 259–266 (2006).
7. J. Ye, L. Lagae, G. Maes, G. Borghs, and P. Van Dorpe, "Symmetry breaking induced optical properties of gold open shell nanostructures," Opt. Express **17**(26), 23765–23771 (2009).
8. S. Mukherjee, H. Sobhani, J. B. Lassiter, R. Bardhan, P. Nordlander, and N. J. Halas, "Fanoshells: nanoparticles with built-in Fano resonances," Nano Lett. **10**(7), 2694–2701 (2010).
9. M. Wickenhauser, J. Burgdörfer, F. Krausz, and M. Drescher, "Time resolved Fano resonances," Phys. Rev. Lett. **94**(2), 023002 (2005).
10. F. Hao, P. Nordlander, Y. Sonnefraud, P. V. Dorpe, and S. A. Maier, "Tunability of subradiant dipolar and fano-type plasmon resonances in metallic ring/disk cavities: implications for nanoscale optical sensing," ACS Nano **3**(3), 643–652 (2009).
11. X. R. Su, Z. S. Zhang, L. H. Zhang, Q. Q. Li, C. C. Chen, Z. J. Yang, and Q. Q. Wang, "Plasmonic interferences and optical modulations in dark-bright-dark plasmon resonators," Appl. Phys. Lett. **96**(4), 043113 (2010).
12. H. Wang, Y. Wu, B. Lassiter, C. L. Nehl, J. H. Hafner, P. Nordlander, and M. J. Halas, "Symmetry breaking in individual plasmonic nanoparticles," Proc. Natl. Acad. Sci. U.S.A. **103**(29), 10856–10860 (2006).

#140227 - $15.00 USD Received 3 Jan 2011; revised 28 Jan 2011; accepted 12 Feb 2011; published 1 Mar 2011

13. K. Bao, N. A. Mirin, and P. Nordlander, "Fano resonances in planar silver nanosphere clusters," Appl. Phys., A Mater. Sci. Process. **100**(2), 333–339 (2010).
14. J. A. Fan, K. Bao, C. Wu, J. Bao, R. Bardhan, N. J. Halas, V. N. Manoharan, G. Shvets, P. Nordlander, and F. Capasso, "Fano-like interference in self-assembled plasmonic quadrumer clusters," Nano Lett. **10**(11), 4680–4685 (2010).
15. J. B. Lassiter, H. Sobhani, J. A. Fan, J. Kundu, F. Capasso, P. Nordlander, and N. J. Halas, "Fano resonances in plasmonic nanoclusters: geometrical and chemical tunability," Nano Lett. **10**(8), 3184–3189 (2010).
16. M. Hentschel, M. Saliba, R. Vogelgesang, H. Giessen, A. P. Alivisatos, and N. Liu, "Transition from isolated to collective modes in plasmonic oligomers," Nano Lett. **10**(7), 2721–2726 (2010).
17. M. Aeschlimann, M. Bauer, D. Bayer, T. Brixner, F. J. García de Abajo, W. Pfeiffer, M. Rohmer, C. Spindler, and F. Steeb, "Adaptive subwavelength control of nano-optical fields," Nature **446**(7133), 301–304 (2007).
18. L. Verslegers, P. B. Catrysse, Z. Yu, and S. Fan, "Deep-subwavelength focusing and steering of light in an aperiodic metallic waveguide array," Phys. Rev. Lett. **103**(3), 033902 (2009).
19. P. K. Jain, X. Huang, I. H. El-Sayed, and M. A. El-Sayed, "Noble metals on the nanoscale: optical and photothermal properties and some applications in imaging, sensing, biology, and medicine," Acc. Chem. Res. **41**(12), 1578–1586 (2008).
20. P. B. Johnson, and R. W. Christy, "Optical constants of the noble metals," Phys. Rev. B **6**(12), 4370–4379 (1972).
21. D. W. Brandl, N. A. Mirin, and P. Nordlander, "Plasmon modes of nanosphere trimers and quadrumers," J. Phys. Chem. B **110**(25), 12302–12310 (2006).
22. A. Christ, O. J. F. Martin, Y. Ekinci, N. A. Gippius, and S. G. Tikhodeev, "Symmetry breaking in a plasmonic metamaterial at optical wavelength," Nano Lett. **8**(8), 2171–2175 (2008).
23. N. Liu, L. Langguth, T. Weiss, J. Kästel, M. Fleischhauer, T. Pfau, and H. Giessen, "Plasmonic analogue of electromagnetically induced transparency at the Drude damping limit," Nat. Mater. **8**(9), 758–762 (2009).
24. S. A. Maier, "Plasmonics: The benefits of darkness," Nat. Mater. **8**(9), 699–700 (2009).
25. C. L. Garrido Alzar, M. A. G. Martinez, and P. Nussenzveig, "Classical analog of electromagnetically induced transparency," Am. J. Phys. **70**(1), 37–41 (2002).

1. Introduction

The existence of Fano Resonances (FRs) in metallic nano-structures has generated considerable interest [1, 2]. At the same time, advancements in nano-fabrication techniques enable the study of complex metallic nano-structures and their plasmonic properties. In order to study the dynamics of the FR in nanoscale optical systems, many studies have been recently undertaken to investigate collective plasmon modes arising from the interaction among individual components of nano-structures [3–5]. Many aspects of the emergence of FRs can be well explained via simple harmonic oscillator models [6]. FRs in nanoscale plasmonic systems have been obtained with symmetry breaking [7, 8], breaking of time reversal symmetry [9], fabricating multiple metallic elements [3] or tuning of incidence angle [10] and light polarization [11]. These asymmetric conditions allow high-order multipolar modes to couple directly with normal incident light. It leads to a destructive interference among the multi-polar and the dipolar modes, which results in FR generation [12]. Meanwhile, FR in planar symmetrical structures [13], such as quadrumers [14] and heptamers [5, 15, 16] has been investigated via anti-parallel coupling of the dipolar modes. However, the low ratio of the anti-parallel to the parallel dipoles arising from the individual components in these structures attributed to relatively weak FR.

In this paper, arrays of plasmonic pentamers consisting of five metallic nano-disks of same size were designed and fabricated. In order to explore the plasmon interactions among these five disks and their optical properties, arrays of plasmon monomers and ring-like quadrumers were fabricated and characterized as well. It was found that in relation to previous studies of heptamers, reduction in the number of surrounding disks leads to an enhancement in the ratio of anti-parallel dipoles to the parallel dipoles, which generates a stronger FR at normal light incidence, unlike to heptamers in which the objective characteristics were angle of incidence ~50° because of the retardation effects in heptamer structures [15]. Meanwhile, it is demonstrated that interference between collective plasmon modes in pentamers leads to a unique optical energy distribution. In order to tune the field localization at the nanoscales, different approaches have been developed recently, such as applying phase shift in co-illumination by two light sources or angled incidence [11, 17]. Here we show that the

#140227 - $15.00 USD Received 3 Jan 2011; revised 28 Jan 2011; accepted 12 Feb 2011; published 1 Mar 2011

polarization direction in the pentamer geometry can be a versatile tool to tune the position of localized electric field enhancement on the nanometer scale, keeping in mind that the pentamer structure is isotropic in plane and collective optical properties are independent of polarization. This could realize various applications in nanolithography [18], nanoscale sensing and medical diagnostics [19].

2. Experimental

Arrays of pentamers, ring-like quadrumers and monomers, were fabricated by electron beam lithography (Elonix 100KV EBL system) on silicon and quartz substrates to investigate reflection and transmission responses, respectively. A 3 nm thick Ti film was first deposited by e-beam evaporation (EB03 BOC Edwards) on the substrates to increase the Au adhesion followed by 60 nm Au film. Subsequently hydrogen silsesquioxane (HSQ) as a negative electro-resist (thickness: 50 nm) was spin coated. The samples were baked at ~200 °C for 120 seconds. After exposure and develop, the nano-structures on the electro-resist were transferred down to the Au films by ion milling. To characterize the fabricated samples, a UV-Vis-NIR micro spectrophotometer (CRAIC QDI 2010 based on a Leica DMR microscope) was used. A normal incident light with x- and y- linear polarizations was applied to excite the structures. Simulated curves were obtained by a three-dimensional finite-difference time domain technique (FDTD) using a perfectly matched layer (PML) around the structures in the wavelength range of 300 ~1300 nm. The dielectric functions used for the simulation was obtained from the experimental data of Johnson and Christy [20].

3. Results and discussion

The pentamer nano-structure under consideration is illustrated in Fig. 1(a). The monomer and ring-like quadrumer are the constituent components of the pentamer. Monomer and quadrumer arrays of the same sizes as those in the pentamer array were fabricated for comparison and analyses. Figures 1(b) and (d) show the SEM images of three periodic patterns of monomers, quadrumers and pentamers fabricated on the silicon substrates. The diameter and height of disks are 142 ± 2 nm and 60 ± 4 nm, respectively and the gap between disks in pentamers is 18 ± 2 nm. Since the arisen plasmons are extremely sensitive to the shapes of structures, significant efforts have been made to fabricate well shaped nano-disks with low size variation.

#140227 - $15.00 USD Received 3 Jan 2011; revised 28 Jan 2011; accepted 12 Feb 2011; published 1 Mar 2011

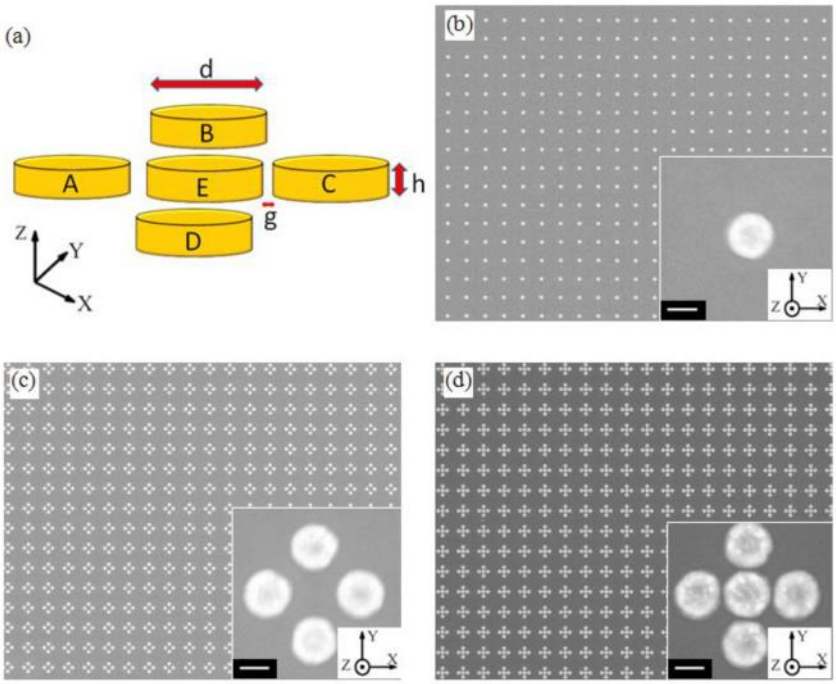

Fig. 1. (a) Sketch of pentamer arrays. SEM images of periodic array patterns of (b) monomers, (c) ring-like quadrumers and (d) pentamers. Scale bar is 100 nm.

In order to gain physical insight into the coupling among nano-disks, the optical responses of plasmonic monomers, quadrumers and pentamers were simulated as results are shown in Fig. 2(a). The measured transmission spectra of the structures fabricated on the quartz substrates are displayed in Fig. 2(b). Apart from a red shift due to the absence of substrate in the simulation, measured and simulated spectra show good agreement. The transmission spectra of the Au monomers and ring-like quadrumers plotted in Figs. 2(a) and (b) reveal the excitation of dipolar mode, with a symmetric Lorentzian profile. Meanwhile, the transmission dip of the quadrumer spectrum is deeper than that of the monomer spectrum due to existence of more nano-disks on the substrate. From the transmission spectra, it can also be observed that the ring-like quadrumer structure behaves similarly to the isolated monomer due to the well-separated configuration of the nano-disks. It can be observed from the orientation of charge distributions in the quadrumer before and after the resonance as shown in Figs. 2(c) and (d) around the wavelengths of 500 nm and 650 nm, respectively. These charge distributions display that the plasmons in the disks A, B, C, and D oscillate in phase, leading to the excitation of a broad super-radiant bright mode centered around 575 nm, where the direction of oscillation gets reversed. However, previous studies have shown that symmetry breaking in nano-shell quadrumers and reducing the gap between two central particles down to 2 nm, may lead to the appearance of anti-parallel dipole moments at certain polarization direction, between the two central nano-particles oppose those of the top and bottom with highly polarization-dependent optical responses [14]. Generally in planar oligomers the super-radiant bright mode comes to existence when the plasmons of all the nano-disks or particles oscillate in phase. While the signature of the sub-radiant mode becomes apparent when the opposite anti-parallel dipolar moments appear [15, 16] leading to a reduction in net dipole moment and hence a diminished coupling to incident light.

#140227 - $15.00 USD Received 3 Jan 2011; revised 28 Jan 2011; accepted 12 Feb 2011; published 1 Mar 2011

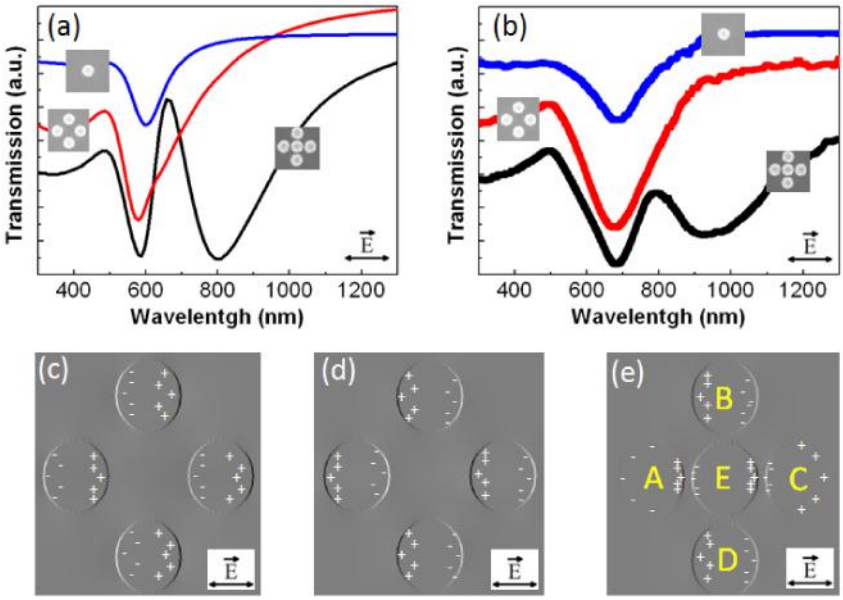

Fig. 2. (a) Simulated and (b) experimental transmission spectra of monomers, quadrumers and pentamers at x-polarized normal incidence. Calculated charge distribution for the ring-like quadrumer (c) before the resonance at 500 nm and (d) after the resonance 650 nm and (e) Charge distribution of the pentamers structure at a wavelength of 665 nm.

While the fabricated quadrumers in this work generate only a polarization-independent broad dipole resonance because of its high degree of symmetry [21], a unique spectral feature appears when a central nano-disk is introduced into the center of the ring-like quadrumer to form pentamer structure. In this case, the dipolar plasmon, arising from the central disk, hybridizes with the ring-like quadrumer dipolar plasmons, allowing the formation of a dark sub-radiant collective mode in addition to the bright super-radiant collective mode [22]. In pentamers, it is obtained while the optical properties are kept polarization-independent due to the in-plane isotropic nature of the pentamer unlike to asymmetric quadrumers [14]. The charge distribution pattern in a single pentamer at a wavelength of 665 nm is plotted in Fig. 2(e). It shows the configuration of anti-parallel modes where disks A, E, and C oscillate in the opposite phase with respect to disks B and D. The effect of the anti-parallel dipolar modes in the pentamers leads to the formation of the sub-radiant mode. It can be observed from the transmission spectra in an asymmetric line-shape known as FR around 665 nm in Fig. 2(a) and around 770 nm in Fig. 2(b). The existence of FR in the pentamers demonstrates that the condition of destructive interference effects between the sub-radiant mode and the supper-radiant mode is sufficiently fulfilled. It is worth mentioning that reduced net dipole moment in pentamers accompanied by reducing losses in the metal can lead to the emergence electromagnetically induced transparency (EIT)-like resonances, as well [23].

Since the central nano-disk substantially dictates the transition from the isolated to the collective modes and plays a crucial role for the formation of the FR, it can be concluded that such kinds of designs have the ability to switch on and off the FR in totally symmetric conditions either by adding or removing the central nano-disk [16]. Heptamers, another planar symmetric structures in which FR can be exhibited, have been studied recently [15, 16]. But it is noticeable that in heptamers, the destructive interference between the super-radiant and the sub-radiant modes happens when the net sum of the plasmons of the six outer disks oscillates oppositely with respect to the plasmon arising from the central nano-disk [15, 16]. Since the formation of the distinct Fano-line shape in the spectrum is due to this destructive interference, the contrast of the FR in the heptamers is lower than the FR investigated in this

#140227 - $15.00 USD Received 3 Jan 2011; revised 28 Jan 2011; accepted 12 Feb 2011; published 1 Mar 2011

paper. In other words, in the heptamers the dipole moment arising from the central disk is weaker as compared to collective opposite mode resulting from the six outer disks. But in this work, it is found that when the number of outer disks is reduced from six to four, the ratio value between two collective opposite modes increases. It is a result of changing the ratio between the opposing phase oscillating plasmons from 1/6 in the heptamers to 2/3 in the pentamers as shown in Fig. 2(e). The FR can be seen obviously in the experimental spectra in Fig. 2(b). It can promote the efficiency of biological and chemical detection [1].

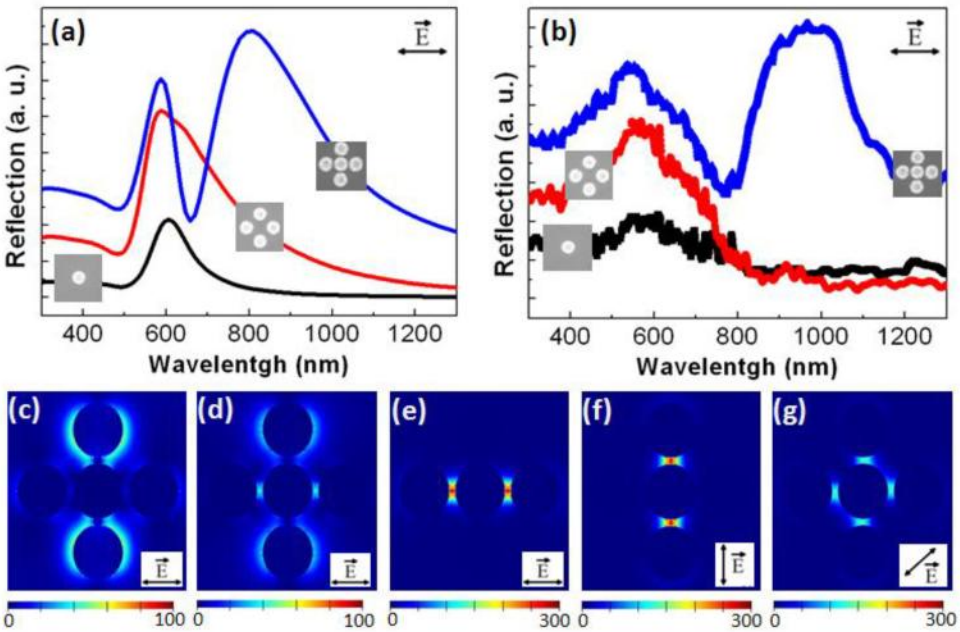

Fig. 3. (a) Simulated and (b) experimental reflection spectra of the monomers, quadrumers and pentamers at x-polarized normal incidence. Calculated field distribution at x-polarized normal incidence at the wavelengths of (c) 585 nm, (d) 670 nm and (e) 805 nm and at a wavelength of 805 nm and at (f) y-polarized and (g) 45-degree polarized light incidence.

For our fabricated pentamers, pronounced Fano-minimum can be observed in reflection responses as well. To measure the reflection mode, the arrays of monomers, quadrumers and pentamers of the same sizes and configuration were fabricated on the silicon substrates. Figures 3(a) and (b) show the reflection spectra of these structures by simulation and experiment, respectively. The presence of the collective dipolar plasmon resonances in the monomers and quadrumers are the same as those shown in the transmission spectra in Fig. 2. Meanwhile, the Fano-line shape can be seen in the pentamer reflection spectrum as well. Figure 3 reveals that the reflection results also possess a good qualitative agreement with the simulated results. In order to elucidate the character of the resonances, electric field distributions for the Au pentamers in various wavelengths are shown in Figs. 3(c) to (g). Distribution of field intensity corresponding to the collective dipolar moments is plotted in Figs. 3(c) and (e) at 585 nm and 805 nm, respectively. The field distribution corresponding to the maximum destructive interferences of the sub-radiant and super-radiant modes can be seen in Fig. 3(d) at 670 nm, where the effect of destructive interference on the value of both dipolar moments leads to the emergence of Fano line-shape in the reflection spectrum. An interesting feature in this design is its unique spatial electric field distribution and light amplification. Figure 3(e) shows how the pentamer is able to concentrate light down to sub-20 nm gaps at the wavelength of 805 nm. This plot displays the local field intensity redistribution within the gaps among the central disk and disks A and C of the pentamer at x-polarized

#140227 - $15.00 USD Received 3 Jan 2011; revised 28 Jan 2011; accepted 12 Feb 2011; published 1 Mar 2011

illumination. The field intensity shows hundreds-fold increase only inside the gaps which reveals that these separated disks can be used as an optical antenna. Meanwhile, Figs. 3(f) and (g) show the pentamer structures at y-polarized and 45 degree-polarization (in X-Y plane) illumination, respectively. These plots demonstrate that the field can be strongly localized in the left and right gaps under x-polarized excitation, but in the top and bottom gaps under y-polarized excitation and in these four gaps under a 45-degree polarization. It is the unique feature of the pentamers to store light energy in different positions selectively by changing the polarization. Keeping in mind that the total amount of re-distributed field intensities which are shown in Figs. 3 (c) to (g) kept constant during changing the polarization orientation. For spatial control over the nanoscopic field distribution, this structure does not require co-illumination by two light sources [11] and the adjustment of the phase delay between them [11, 17]. This advantage benefits potential applications for plasmon-based all optical information processing [11] and control of light matter interactions in the nanoscales [24].

Optical responses of the pentamers can be explained by a spring-mass model [6, 25] which consists of five coupled interacting oscillators illustrated in Fig. 4(a). According to the field distribution plots in Figs. 3(c) to (g), two hypotheses are argued. Firstly, the springs among the outer disks in the oscillator system are neglected since the outer disks in the pentamers do not have considerable interactions between each other. This can be inferred from the transmission spectra of the quadrumers in Fig. 2 where a dipole resonance identical to the monomer is seen. Secondly, the interacting system of the five coupled oscillators can be simplified to a three coupled interacting oscillators system, because the coupling among disks A and C with respect to disk E are similar, as well as disks B and D with respect to disk E. Figure 4(b) displays the simplified system in which mass 1 represents disk E, mass 2 represents disks A and C, and mass 3 represents disks B and D. This model is an extension of the classical two oscillators system which was used to study the nature of FR [6] and three oscillator system as the analogous of Fano-shell structures [8]. In Fano-shell model, all three oscillators are connected to each other because of direct effect of dipole, quadrupole and dark modes on each other, under optical excitation. But in the model presented in this work the spring between oscillators 2 & 3 are neglected since the interaction of ring-like disks in pentamers are neglectable and each of surrounding disks just approach the central disk individually and directly during optical excitation.

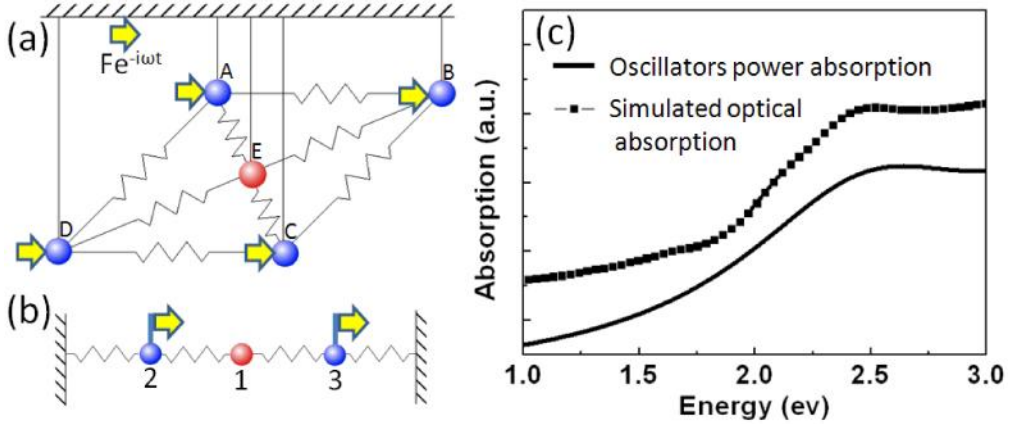

Fig. 4. (a) Five coupled interacting oscillators representing the pentamer optical responses, (b) simplified three coupled oscillators and (c) simulated plasmons absorption spectra by FDTD (dot line) and calculated power absorption in the oscillator model (solid line).

The mass values in this model are assumed as $m_1=m_2=m_3=1$ and all springs are the same. As explained before, the dark mode is a result of adding the central disk. Therefore outer oscillators are taken to be driven by a harmonic force $\mathbf{F}(t)= \mathbf{F}e^{-i\omega t}$ as the bright mode

#140227 - $15.00 USD Received 3 Jan 2011; revised 28 Jan 2011; accepted 12 Feb 2011; published 1 Mar 2011

exhibitors. Subsequently, in the simplified system the oscillators 2 and 3 are taken to be driven by a harmonic force. It is unlike to Fano-shell mechanical model [8] in which the dipole bright mode is assumed as the responsible for exciting the quadrupolar mode and subsequently sub-radiant dark mode and only one oscillator is driven by harmonic force. For coupled oscillators model in this work, the motion equations of oscillators |1>, |2> and |3> are solved in terms of displacements x_1, x_2 and x_3 from the equilibrium positions:

$$\ddot{x}_1(t) + \gamma_1 \dot{x}_1(t) + \omega_1^2 x_1(t) - \Omega^2 x_2(t) - \Omega^2 x_3(t) = 0, \quad (1)$$

$$\ddot{x}_2(t) + \gamma_2 \dot{x}_2(t) + \omega_2^2 x_2(t) - \Omega^2 x_1(t) = Fe^{-i\omega t}, \quad (2)$$

$$\ddot{x}_3(t) + \gamma_3 \dot{x}_3(t) + \omega_3^2 x_3(t) - \Omega^2 x_1(t) = Fe^{-i\omega t}, \quad (3)$$

where $\boldsymbol{\omega_1}$, $\boldsymbol{\omega_2}$ and $\boldsymbol{\omega_3}$ are oscillation frequencies, corresponding to the oscillators 1, 2, and 3, respectively, and $\boldsymbol{\Omega}$ coherent coupling frequencies between interconnected oscillators which represents the coupling between anti-parallel modes in the optical system. $\boldsymbol{\gamma_1}$, $\boldsymbol{\gamma_2}$ and $\boldsymbol{\gamma_3}$ are the friction coefficients which are used to account for the energy dissipation of |1>, |2> and |3>, respectively. These friction coefficients represent the dissipated energy among nano-disks during energy transformation at optical excitation. By tuning the coupling between bright mode and dark mode ($\boldsymbol{\Omega^2}$=1.69) and other parameters ($\boldsymbol{\omega_1}$ =2.5 eV, $\boldsymbol{\omega_2}$ =3.1 eV, $\boldsymbol{\omega_3}$ =5 eV, $\boldsymbol{\gamma_1}$=1, **@003@004@005** $\boldsymbol{\gamma_2}$ **@003@005**=42E-2, $\boldsymbol{\gamma_3}$ =20E-2 and F=10), the absorption power of the oscillator system reproduces the optical absorption of the pentamer. Figure 4(c) shows the comparison between absorbed powers of the oscillator system calculated by Eqs. (1) to (3) with the FDTD simulated plasmon response of the pentamer. As it was seen in Figs. 2(a) and 3(a), in pentamers the reflection and the transmission spectra posses almost a reverse trend. Consequently the absorption spectrum does not experience a pronounced peak as can be seen in Fig. 4(c). However it keeps increasing with the rise of the energy. The trend which is almost reproduced by absorption response of the classical oscillators model.

Conclusions

In summary, a five same nano-disk pentamer exhibiting a high contrast FR is investigated. The FR was obtained under normal incident light along all orientations of polarization. It was demonstrated that the monomers and the ring-like quadrumers behave the same as the isolated nano-disks exhibiting only the isolated mode. After the addition of the central disk into the center of the quadrumers to form the pentamers, an anti-parallel coupling of dipolar modes appears. The ratio between anti-parallel and parallel dipole modes is 2/3 and results in the generation of a pronounced FR as compared to the other planar symmetric structures. The existence of a FR in the pentamers was explained by the mass-spring oscillator model. Meanwhile, the polarization orientation is found to be an efficient tool to tune the localization of the electromagnetic intensity in nanoscales. It was shown that the pentamer can manipulate light in a sub-diffraction length scale and overcome the spatial restrictions of conventional optics. The tuning of light spatial distribution can be achieved by only a single source, instead of applying a phase shift in a co-illumination system.

Acknowledgements

The authors would like to acknowledge the funding provided by SERC Agency of Science, Technology And Research (A*STAR) Superlens Program (Project No. 092 154 0099) for the research work published in this paper. In addition the authors thank Professor Stefan A. Maier and Dr. Dang Yuan Lei for useful discussion and comments. Mohsen Rahmani would like to express his gratitude for the support from the A*STAR – SINGA scholarship program.

#140227 - $15.00 USD Received 3 Jan 2011; revised 28 Jan 2011; accepted 12 Feb 2011; published 1 Mar 2011